

## Factors affecting waterproof efficiency of grouting in single rock fracture

Hang Bok Lee<sup>1a</sup>, Tae-Min Oh<sup>\*1</sup>, Eui-Seob Park<sup>1b</sup>,  
Jong-Won Lee<sup>2c</sup> and Hyung-Mok Kim<sup>2d</sup>

<sup>1</sup> Center for Deep Subsurface research, Korea Institute of Geoscience and Mineral Resources,  
Daejeon 305-350, Republic of Korea

<sup>2</sup> Department of Energy & Mineral Resources Engineering, Sejong University,  
Seoul 143-747, Republic of Korea

(Received October 07, 2016, Revised December 05, 2016, Accepted February 14, 2017)

**Abstract.** Using a transparent fracture replica with aperture size and water-cement ratio (w/c), the factors affecting the penetration behavior of rock grouting were investigated through laboratory experiments. In addition, the waterproof efficiency was estimated by the reduction of water outflow through the fractures after the grout curing process. Penetration behavior shows that grout penetration patterns present similarly radial forms in all experimental cases; however, velocity of grout penetration showed clear differences according to the aperture sizes and water-cement ratio. It can be seen that the waterproof efficiency increased as the aperture size and w/c decreased. During grout injection or curing processes, air bubbles formed and bleeding occurred, both of which affected the waterproof ability of the grouting. These two phenomena can significantly prevent the successful performance of rock grouting in field-scale underground spaces, especially at deep depth conditions. Our research can provide a foundation for improving and optimizing the innovative techniques of rock grouting.

**Keywords:** waterproof efficiency; penetration pattern; rock grouting; aperture sizes; water-cement mixed ratio (w/c)

### 1. Introduction

Various underground facilities have recently been required to store energy (e.g., oil storage) and waste (e.g., radioactive waste) at deep depth (Gueddouda *et al.* 2010, Wang *et al.* 2015). For construction of such underground facilities at deep depth, rock grouting is an important reinforcement method to prevent the water leakage. Without the appropriate grouting waterproof in the underground facilities, structure stability and storage ability cannot be guaranteed (Chun *et al.* 2006, Axelsson *et al.* 2009, Butrón *et al.* 2009, Lisa *et al.* 2012, Rafi and Stille 2014, Zhang *et al.* 2017).

---

\*Corresponding author, Senior Researcher, E-mail: tmoh@kigam.re.kr

<sup>a</sup> Senior Researcher, E-mail: leehb@kigam.re.kr

<sup>b</sup> Principal Researcher, E-mail: espark@kigam.re.kr

<sup>c</sup> Graduate Student, E-mail: leelee6733@naver.com

<sup>d</sup> Associate Professor, E-mail: hmkim@sejong.ac.kr

For rock grouting, the grout materials are mixed with water for flowing, and injected into the drilled boreholes. The slurry grout migrates through individual fractures that are cross-connected with field boreholes; finally, the grout fills the fracture networks near the underground structure. For this method to work as a successful waterproof mechanism, the grout material has to have the ability to flow well in rock fractures and to achieve proper strength after curing. Understanding of grout penetration behavior is very important in relation to waterproof efficiency of rock grouting because the sealing of narrow fractures is dependent on the ability of the injected grout to penetrate into the fractures, especially at deep depth condition (Fuenhag and Fransson 2006, Chegbeleh *et al.* 2009, Saeidi *et al.* 2013, Mohajerani *et al.* 2015, Mohammed *et al.* 2015).

Therefore, in order to achieve an economical and efficient design of rock grouting at deep depth, the performance should be verified according to the grout properties, the geometry of the fractures, and underground ambient environmental conditions such as the water saturation level or temperature (Gustafson and Stille 1996, Sui *et al.* 2015). Several researchers have studied grouting efficiency for fractured rock and its relationship with grout penetration into individual fractures. Eriksson (2002a, b) concluded that the aperture size, its variation, and geometrical measures are the most important factors affecting grout penetrability. Draganovic and Stille (2011) also suggested that many factors such as grout pressure, density, and the geometry of constriction can influence the complex process of injected grout penetration. The effect of flowing water on grouting in fractured rock was experimentally investigated by Zhang *et al.* (2011). Recently, Sui *et al.* (2015) evaluated the relationship between sealing efficiency and influencing factors such as fracture aperture width, initial water velocity, gel time, and grout take in a single fracture model. However, they did not analyze the specific mechanism causing the differences of waterproof efficiency and grout penetration behavior including penetration pattern or velocity. In addition, they did not consider the influence of high water pressure on the waterproof ability of rock grouting in relation to deep depth condition.

In this study, both grouting injection and waterproof tests were performed using micro cement grout in a transparent fracture replica with various aperture sizes and w/c ratios. Given the experimental data, penetration behavior of grout was first analyzed according to aperture sizes and w/c ratios; then, factors affecting the waterproof efficiency were evaluated through water permeability tests with high water pressure. In addition, the phenomena of air bubbles that formed and bleeding that occurred during injection or curing of grout were discussed for the successful performance of rock grouting. The results of this study can provide basic knowledge to determine the efficiency of waterproofing for rock grouting at deep depth.

## 2. Materials and methods

### 2.1 Material used in experiments

Micro cements are often used to improve the strength of poor rock and to prevent ground water inflow into underground spaces (Eriksson 2002a, b, Chun *et al.* 2006, Northcroft 2006, Panthi and Nilsen 2010, Stille *et al.* 2012, Høien and Nilsen 2014, Khavé 2014). At deep depth conditions, the aperture sizes of individual fractures are very small due to high in-situ stress (Saberhosseini *et al.* 2014, Zhu *et al.* 2014). Thus, ordinary cement has a limitation as a grout material to be injected into fine rock joint. For this reason, the grout material selected for our experiments is MICEM 8000 (micro cement), manufactured by SsangYong cement in Korea. Fig. 1 and Table 1 provide the grain size distribution and physical properties of MICEM 8000 (SsangYong cement Inc. 2016).

Table 1 Physical properties of micro grout (MICEM 8000) (SsangYong cement Inc. 2016)

Property	Value
Specific gravity (-)	2.95
Particle size of $D_{95}$ ( $\mu\text{m}$ )	< 16
Average particle size ( $\mu\text{m}$ )	4 – 6

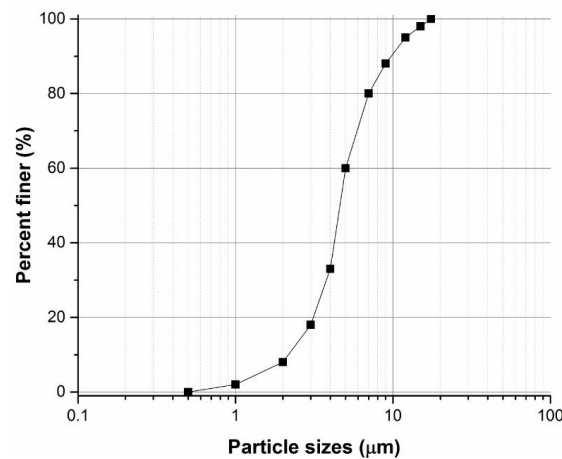


Fig. 1 Grain size distribution curve of micro grout (MICEM 8000) (SsangYong cement Inc. 2016)

The micro cement used in this study has a  $D_{95}$  of less than  $16 \mu\text{m}$  for grain size distribution and a specific gravity of 2.95 (Fig. 1). Water-cement mixed ratio (w/c) is an important factor for characterizing the viscous fluid flow in rock fractures. Previous studies mainly used a w/c range from 0.5 to 1.0 (Chun *et al.* 2002, Høien and Nilsen 2014, Rahman *et al.* 2015). Considering the bleeding and fluidity of grout, the w/c values were divided into categories of low and high. Low w/c was determined to be a value of 0.6 of w/c; high w/c was determined to be a value of 1.0. Viscosity values of low w/c (0.6) and high w/c (1.0) were obtained at 327 and 22 centipoise (cP), respectively (water viscosity is 1 cP for reference). A centipoise (cP) is a non-SI (non-System International) measurement unit of dynamic viscosity in the centimeter gram second (CGS) system of units. A centipoise is equal to one millipascal-second (mPa·s) in SI units. Low and high w/c values showed an approximately 15 times difference of viscosity value. The chemical additives for hardening and improving grout were not considered in this experiment.

Fig. 3 shows a test cell for evaluating the penetration behaviors and waterproof efficiency of grouting in a single rock fracture. The cell was a specially designed rectangular acrylic parallel plane model and had a fracture size of 200 mm (width)  $\times$  400 mm (length) with different apertures (1, 5, and 10 mm). The International Society for Rock Mechanics (ISRM 1978) suggested that fractures with apertures between 0.5 and 10 mm are possible pathways for flowing water in grouting practice. Thus, fracture cells with aperture sizes of: 1–10 mm were selected and used in this experiment. To describe the deep underground space and the permeability estimation (A and C), the ports are composed of a grout injection point (B), and water injection and drainage points for initial water saturation conditions. Inner diameter of all ports and distance between ports are 0.95 mm (3/8 inches) and 180 mm respectively. The boundary of the cell was perfectly sealed and thus injected water and grout can only migrate through the ports.



Fig. 2 Micro cement material for grouting injection

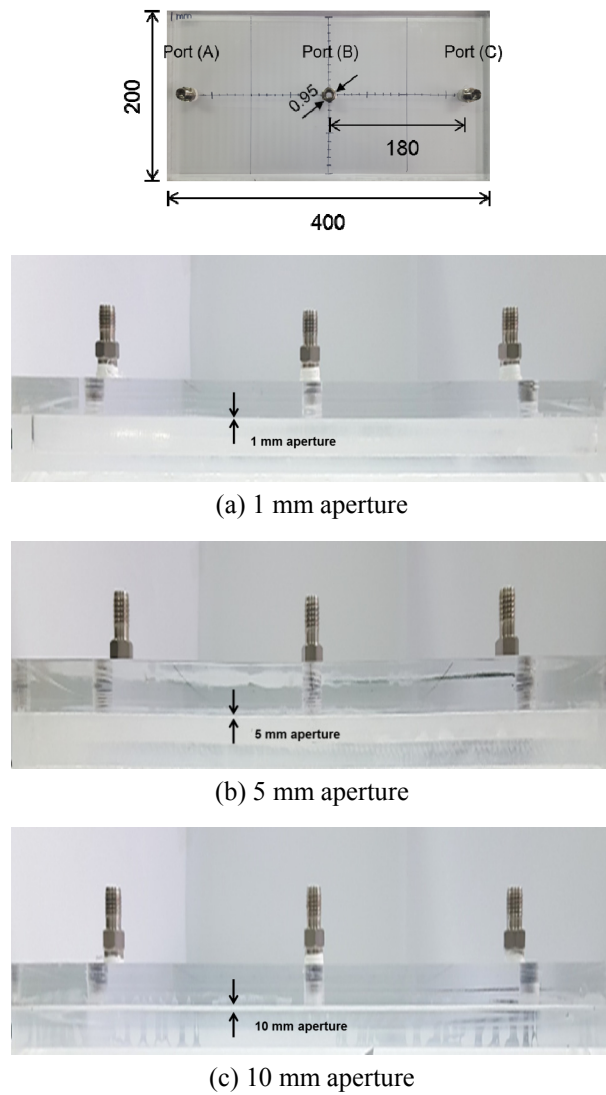


Fig. 3 Test cells of artificial fracture with different aperture and inlet/outlet ports (plane & side view)

## 2.2 Experimental setup and procedures

The total set of laboratory experiments were divided into two parts: a grout injection test to evaluate the penetration behaviors (i.e., pattern and velocity) and a permeability test to evaluate the waterproof efficiency after curing. Fig. 4 shows the total experimental setup for the grout injection and permeability test in deep underground conditions; it is composed of four parts: the syringe pump, the high pressure pump, the data acquisition system, and the test section.

In this experiment, the syringe pump was used to inject grout into the artificial fracture. The dynamic flow rate provided by the syringe pump was able to reach 6000 mL/min. A high-pressure water pump was used to estimate the permeability and waterproof efficiency of the rock grouting. This pump can provide high water pressure of up to 10 MPa. A multichannel data system was installed to control the experimental parameters and to acquire data. Using the display system, we regulated the injection conditions of the pumps such as the injection pressure and flow rate of the fluid materials. Also, the feedback system was used to optimize and stabilize the injection conditions. A digital camera was used to visually observe and record the penetration and distribution of the injected grout. This visual device has a display resolution of  $4608 \times 3288$  (15 million) and can record moving images at 7 frames per second.

For the injecting of the grout material, the micro cement was mixed with water under constant conditions ( $w/c = 0.6$  and  $1.0$ ). To prevent separation between the micro cement and the water before injection, the mixtures were sufficiently stirred for 30 minutes under temperature conditions of  $21 \pm 1^\circ\text{C}$ . Mixing process was performed using the EUROSTAR 200 digital overhead stirrer. Stirring quantity is 100 liter, torque is 200 Ncm and speed range is from 30 to 2000 rpm (rounds per minutes). The stirring time was thirty minutes and rotation speed was 1,200 rpm. After stirring, the mixtures were immediately poured into the grout container and injected into single fracture cell. To simulate the rock fractures saturated by groundwater in the deep underground environment, the fracture cell was fully saturated with tap water (Yoon *et al.* 2015). Grout samples with a flow rate of 200 ml/min were injected into port (B) using syringe pump. Ports (A) and (C) were open because they acted as outlets during the grouting injection process. Additionally, to confirm perfect saturation condition of grout inside the fracture cell, grout was continuously injected until



Fig. 4 Experimental setup for grout injection and permeability test

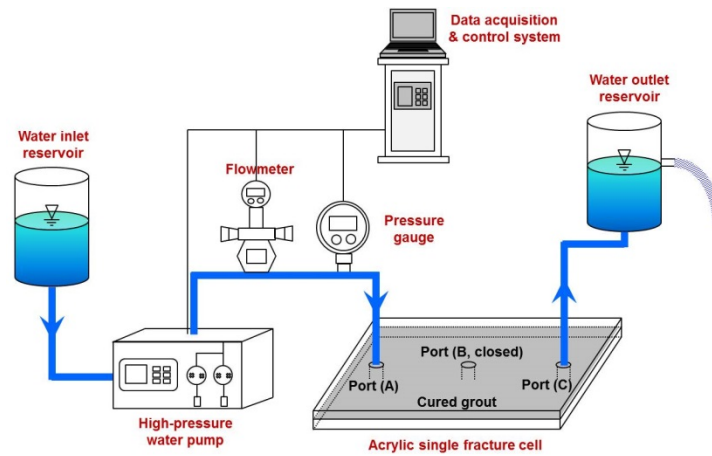


Fig. 5 Procedure for waterproof efficiency test

was pushed out of ports (A) and (C). We used a digital camera to measure the penetration velocity and the distribution of grout.

After grouting, all ports were sealed to prevent external influences while the grouts cured. The curing process proceeded for 7 days at constant temperature of  $21 \pm 1^\circ\text{C}$ . Finally, permeability tests using high-pressure water pump were conducted in the grouted fractures to evaluate the waterproof efficiency of the grouting (Fig. 5). Grout injection port (B) was closed and ports (A) and (C) were set as inlet and outlet, respectively, for the estimating of the water permeability. To estimate the permeability after the curing process, the outflow water at port (C) was collected and measured according to the elapsed time.

### 3. Results and analysis

#### 3.1 Grout penetration behavior

##### 3.1.1 Grout penetration pattern

Fig. 6 shows the penetration patterns of grout injected into fractures with various aperture sizes at  $w/c = 0.6$  and  $1.0$ . Parallel acrylic fractures were initially filled with water. There was no water flow within the fractures; this static water condition was maintained during the grout injection tests. At  $w/c = 1.0$ , the penetration for static water grouting was round in shape during the first 14 seconds before the grout reached the fracture side boundary in the case of the 10 mm aperture size (Fig. 6(a)). In the case of the 5 mm aperture size, an abnormal penetration pattern due to trapped air was observed near the central injection hole (Fig. 6(b)). In the two cases (5 and 10 mm aperture sizes), a circular grout front was commonly observed at the early stage of the grout injection tests. In the case of the small fracture with 1 mm aperture size, the grout radially spreads to both the boundaries of the fracture, but a stratigraphic penetration pattern partially occurs due to the micro-fine furrows and ridges within the fracture formed during the manufacturing process (Fig. 6(c)). Although there were local differences of grout movement, the similar radial penetration pattern was generally identified in all three cases under the no-water flow condition.

At  $w/c = 0.6$ , the same circular shape of grout penetration was also found in the cases of 5 and 10 mm aperture sizes (Figs. 6(d)-(e)). Only a slight dilution was identified in the area between the

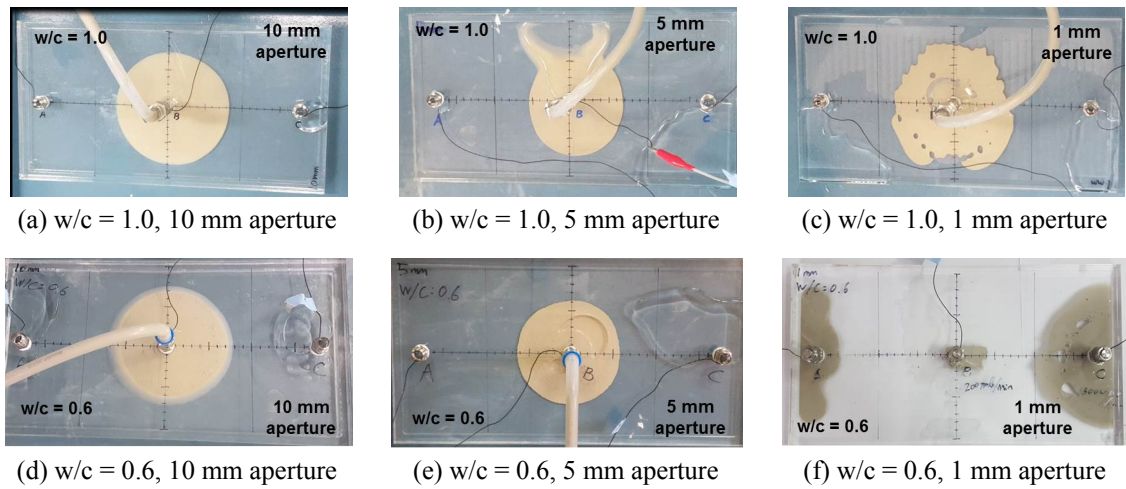


Fig. 6 Penetration patterns of grout

grout body and the saturated water in the case of the 10 mm aperture. However, the grout injected into center port (B) was found rarely to penetrate through the single acrylic fracture and was distributed over a tiny area in the vicinity of port (B) in the case of the 1 mm aperture (Fig. 6(f)). Injection tests for the 1 mm aperture were performed again at ports (A) and (C) with increasing of the injection rate to 3000 ml/min. In spite of the high injection rate, it was observed that the grout penetration was stopped at a very early stage and the final distribution of the injected grout was also limited to the surroundings of ports (A) and (C) (Fig. 6(f)).

### 3.1.2 Grout penetration velocity

Under the condition of constant grout injection rate (200 ml/min), the velocity of grout penetration showed a clear distinction according to the aperture sizes and w/c ratios. In each experimental case, the velocity of the grout penetration was estimated using the penetration distance over the elapsed time.

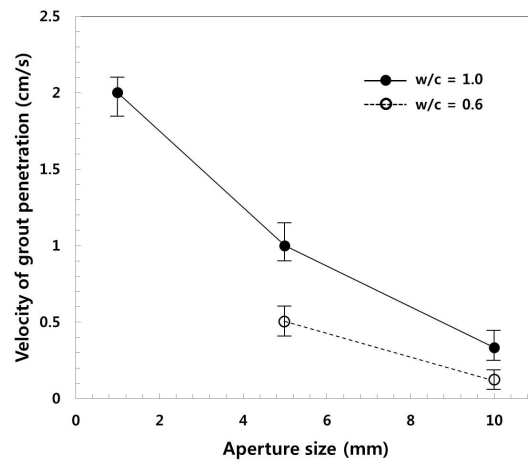


Fig. 7 Velocity of grout penetration at w/c = 0.6 and 1.0 as a function of aperture size

Fig. 7 shows the velocities of grout penetration at  $w/c = 0.6$  and  $1.0$  according to the aperture size. As the aperture size increased, the velocity of grout penetration decreased. The velocities of grout penetration at  $w/c = 1.0$  were found to be 2.0, 1.0, and 0.3 cm/s in the cases of 1, 5, and 10 mm aperture sizes, respectively. The velocities of grout penetration at  $w/c = 1.0$  were inversely proportional to the aperture sizes, which corresponds with the results of the analytical solution suggested by Gustafson and Stille (1996). At  $w/c = 1.0$ , the velocities of grout penetration decreased about 6 times ( $2.0 \rightarrow 0.3$  cm/s) as the aperture size increased 10 times ( $1 \rightarrow 10$  mm), as shown in Fig. 6. However, the velocities of grout penetration decreased 2 times ( $1.0 \rightarrow 0.5$  cm/s) as the viscosity value increased about 15 times ( $22 \rightarrow 327$  cP). This indicates that the effect of the aperture size on the velocity of grout penetration may be greater than that of the viscosity change due to the  $w/c$  ratio. In this regard, sensitivity analysis between the two factors will be needed for more and more various experimental cases, which will lead to a quantitative weighting evaluation of the effects of these factors on grout penetration velocity.

The velocities of grout penetration at  $w/c = 0.6$  were 0.5 and 0.1 cm/s in the cases of 5 and 10 mm aperture sizes, respectively. However, the grout did not penetrate into the fracture with an aperture of 1 mm at  $w/c = 0.6$ . Even under the condition of high injection rate, the injected grout moved only slightly from the injection port to the inside of the fracture, as shown in Fig. 6(f). Thus, the velocity of grout penetration was not properly measured in this case. From this result, we can infer that grout penetration is impossible or very difficult in fine fractures below 1 mm in aperture under  $w/c$  conditions, which may be significantly related to the performance evaluation of grout injection in the real field. To summarize, the velocities of grout penetration at  $w/c = 0.6$  were lower than that at  $w/c = 1.0$  for all aperture sizes. This is because the velocity of grout penetrations increases due to the decrease of grout viscosity with increasing  $w/c$ .

### 3.2 Waterproof efficiency of grouting

To evaluate the waterproof efficiency of grouting, permeability tests were conducted after the curing process. The waterproof efficiency ( $WE$ ) as adopted in this research is defined as the reduction of the cross-fracture flow due to the grouting performance; it can be estimated as follows

$$WE(\%) = \frac{(Q_{initial} - Q_{grouted})}{Q_{initial}} \times 100 \quad (1)$$

where  $Q_{initial}$  is the initial water flow rate before grouting and  $Q_{grouted}$  is the water flow rate after grouting. These values are commonly measured at the outlet port of the fracture. Fig. 8 shows the waterproof efficiency according to the aperture sizes and values of  $w/c$ . At  $w/c = 1.0$ , the waterproof efficiency was found to be 100% after the curing process in the case of the 1 mm aperture size. This means that there was no flow or leakage through the fractures due to grouting in this case, indicating the excellent waterproof efficiency of the grouting. No cracks or water leakage was observed, even at extremely high injected water pressure ( $= 10$  MPa). This implies that the sealing effect of the rock grouting is maintained under deep depth condition ( $\approx 1$  km) in the case of micro-fractures with 1 mm aperture size. In two cases (5 and 10 mm aperture sizes), the waterproof efficiencies were 79.4% and 61.2%, respectively, after the curing process. Although the insides of the fractures were mostly filled with the injected grout for the 5 and 10 mm apertures, empty spaces were widely formed at the upper parts of the fracture channels, which caused water flow even after grout curing. Moreover, the waterproof efficiency was found to decrease as the

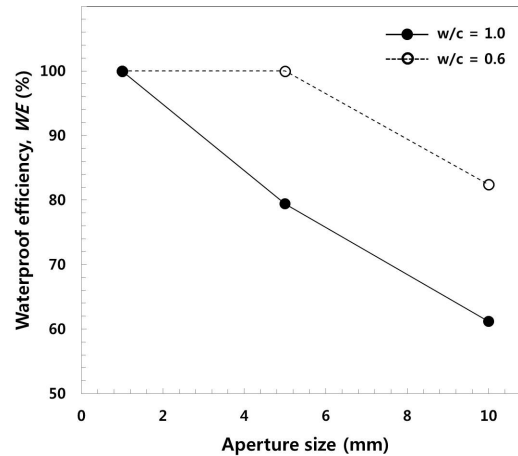


Fig. 8 Waterproof efficiency ( $WE$ ) for  $w/c = 0.6$  and  $1.0$  as a function of aperture size

aperture size increased (Fig. 8). This implies that grouting may not be effective at stopping water flow in fractures with large apertures.

At  $w/c = 0.6$ , the waterproof efficiencies were 100%, 100%, and 82.4% after the curing process in fractures with apertures of 1, 5, and 10 mm, respectively. In the case of the 1 mm aperture, although the injected grout was only distributed around the injection ports, there was no water flow through a single acrylic fracture from the port (A) to (C) during the permeability evaluation tests. This case, however, represents incomplete sealing limited to the vicinity of the injection points, as shown in Fig. 6(f), which can lead to fast reduction of the waterproof efficiency due to crack generation of the grouting in the long term. Therefore, the waterproof efficiency of grouting in the real field should be comprehensively evaluated according to the penetration and distribution of injected grout; water permeability verification must also be performed. Moreover, a long-term permeability test will be needed to identify the continuous waterproof ability of the rock grouting. In the case of the 5 mm aperture, no water flow pathway was observed except in small, separated air pores. We observed the empty space and water flow at the upper part of the fracture channel in the case of the 10 mm aperture. Experimental results showed that the waterproof efficiency was greatly affected by the aperture size and the  $w/c$  value. Consequently, a high waterproof efficiency can be obtained with small apertures and low water-cement mixed ratios ( $w/c$ ).

#### 4. Discussion

When grout is injected into the fracture, air bubbles can form due to the mixing and injection processes. In this study, many air bubbles were observed and separately located inside the fracture, as shown in Fig. 9.

To evaluate the effect of air bubbles on leakage or water permeability after grouting, high pressure water at over 10 MPa was injected into the grouted fracture. Consequently, the separated air bubbles, which act as closed pores, were found not to affect the short-term permeability of fractures sealed by grouting. However, in the case of the grout injection with high pressure at deep depth, more air bubbles may occur due to the formation of turbulent flow. This flow can induce water leakage of the grouted fractures by creating continuous pores. Moreover, the air bubbles may

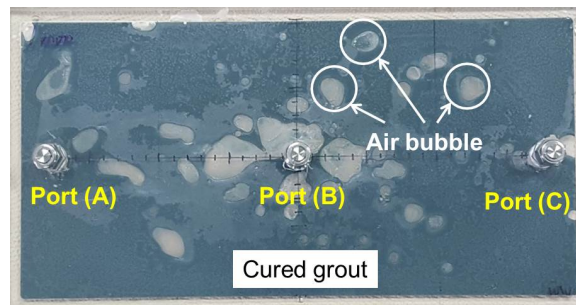


Fig. 9 Example of air bubble occurrence in the grouting process

become large water pathways if the grouting is corroded or deformed in the long-term, which can greatly reduce the grouting efficiency.

Bleeding occurs in the direction of gravity during the curing process after a fracture aperture is fully filled with injected grout, as shown in Fig. 10. This bleeding phenomenon causes empty space at the upper part of a fracture aperture. There are several factors affect the bleeding, also called water separation. Increase of w/c ratio can increase the amount of bleed from the suspension. Generally, the highest w/c ratio used in construction applications is below 2 because of the increased bleeding characteristics and decrease of strength properties. And an increase of the specific surface area (decrease of grain size) of grout particles may reduce water separation due to lower potential for gravitational settlement. Moreover, the fracture geometry (aperture size, roughness, network type and inclination) can affect the pattern or quantity of bleeding.

In this study, there were no gaps between the aperture channels and the cured grout in the case of the 1 mm aperture. In the cases of both the 5 and 10 mm apertures, bleeding was observed at the upper part of the fracture channels (Fig. 10). The ratios of empty space by bleeding to total apertures were 7.4% and 15.2%, respectively. From this result, it can be inferred that the bleeding phenomenon may intensify as the aperture size increases. Water-cement mixed ratio (w/c), as well as the aperture size, can influence the extent of bleeding. In this experiment, when the ratio value was less than 1.0, the bleeding was considerably reduced. However, water flow due to bleeding (6.3%) was still observed in the case of large fractures with 10 mm aperture size, although there was no bleeding in the cases of fractures with apertures of 1 and 5 mm at w/c = 0.6. Therefore, it

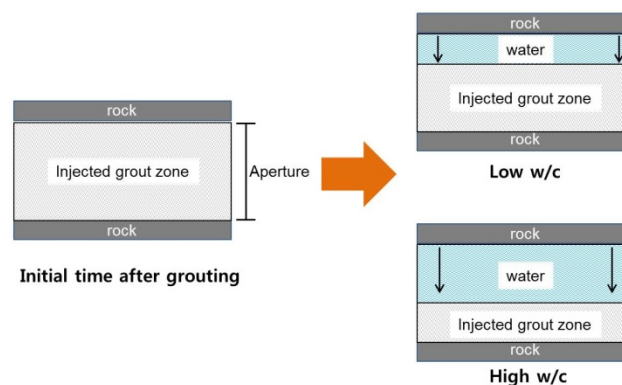


Fig. 10 Bleeding phenomenon in rock fractures with w/c ratio

is important to find an optimal w/c value at which bleeding does not occur according to aperture size, which is closely related to the waterproof efficiency of grouting.

In conclusion, the phenomena of air bubbles and bleeding during injection or curing of grout are major phenomena that decrease the waterproof ability of grouting. Methods to minimize these two phenomena will be needed for the successful performance of rock grouting, especially at deep depth condition. In this respect, we are preparing an expanded study about various other effects of fracture roughness, ambient flow velocity, and temperature on air bubble and bleeding phenomena in real rock fractures. In particular, the ground temperature may be increased up to 60°C at 1 km in deep depth. Generally, high temperature reduces the viscosity of grout fluid, which can cause the increase of fluidity of injected grout. However, the grout is special Bingham fluid having time-dependent property. Temperature increase may affect the curing process of grout, and this can interrupt the grout flow due to the intensification of time-dependency of grout viscosity. Therefore, this complex temperature effects can change grout flow dramatically in deep depth condition, which should be precisely investigated in laboratory-scale injection experiments.

## **5. Conclusions**

In this study, we evaluated the factors affecting the penetration behavior (penetration velocity and pattern) and waterproof efficiency of rock grouting through laboratory experiments using a single transparent fracture replica with various aperture sizes. The main conclusions of our experiments are as follows:

- To achieve efficient waterproofing at deep depth, it is important to obtain fracture aperture information and to determine the w/c ratio; waterproof efficiency increased with a decrease in the fracture aperture and w/c ratio.
- At low w/c (0.6), high waterproof efficiency can be achieved; however, penetration velocity (distance) is low due to high viscosity.
- At high w/c (1.0), long penetration distance can be achieved; however, waterproof efficiency can be low due to the bleeding effect with large aperture size.
- Air bubble and bleeding phenomena can be significantly affected by aperture size and water-cement mixed ratio, and should be considered in rock grouting construction because these factors reduce the waterproof ability especially at deep depth condition.
- Step injection according to w/c ratios (high w/c for long penetration → low w/c for efficient waterproof) are needed in the field according to the fracture conditions (aperture size and crack length).

## **Acknowledgments**

This study was supported by the Basic Research and Development Project of the Korea Institute of Geoscience and Mineral Resources (KIGAM), which was funded by the Ministry of Science, ICT and Future Planning, Korea.

## **References**

Axelsson, M., Gustafson, G. and Fransson, Å. (2009), "Stop mechanism for cementitious grouts at different

- water-to-cement ratios”, *Tunn. Undergr. Space Technol.*, **24**(4), 390-397.
- Butrón, C., Axelsson, M. and Gustafson, G. (2009), “Silica sol for rock grouting: Laboratory testing of strength, fracture behavior and hydraulic conductivity”, *Tunn. Undergr. Space Technol.*, **24**(6), 603-607.
- Chegbeleh, L.P., Nishigaki, M., Akudago, J.A., Alim, M.A. and Komatsu, M. (2015), “Laboratory investigation of ethanol/bentonite slurry grouting into rock fractures: Preliminary results”, *J. Fac. Environ. Sci. Technol.*, **14**(1), 23-28.
- Chun, B.S., Kim, D.Y. and Lee, Y.N. (2002), “Shear characteristic of the cement grouted sawtoothed joints”, *J. Korean Soc. Civil Eng.*, **22**(5C), 469-478.
- Chun, B.S., Lee, Y.N. and Chung, H.I. (2006), “Effectiveness of leakage control after application of permeation grouting to earth fill dam”, *KSCE J. Civil Eng.*, **10**(6), 405-414.
- Draganovic, A. and Stille, H. (2011), “Filtration and penetrability of cement-based grout: Study performed with a short slot”, *Tunn. Undergr. Space Technol.*, **26**(4), 548-559.
- Eriksson, M. (2002a), “Grouting field experiment at the Äspö Hard Rock Laboratory”, *Tunn. Undergr. Space Technol.*, **17**(3), 287-293.
- Eriksson, M. (2002b), “Prediction of grout spread and sealing effect: A probabilistic approach”, Ph. D. Dissertation; Royal Institute of Technology, Stockholm, Sweden.
- Funehag, J. and Fransson, A. (2006), “Sealing narrow fractures with a Newtonian fluid: model prediction for grouting verified by field study”, *Tunn. Undergr. Space Technol.*, **21**(5), 492-498.
- Gueddouda, M.L., Lamara, M., Abou-bekr, N. and Taibi, S. (2010), “Hydraulic behaviour of dune sand-bentonite mixtures under confining stress”, *Geomech. Eng., Int. J.*, **2**(3), 213-227.
- Gustafson, G. and Stille, H. (1996), “Prediction of groutability from grout properties and hydrogeological data”, *Tunn. Undergr. Space Technol.*, **11**(3), 325-332.
- Høien, A.H. and Nilsen, B. (2014), “Rock mass grouting in the Løren tunnel: Case study with the main focus on the groutability and feasibility of drill parameter interpretation”, *Rock Mech. Rock Eng.*, **47**(3), 967-983.
- ISRM (1978), “Suggested methods for the quantitative description of discontinuities in rock masses”, *Int. J. Rock Mech. Min. Sci. Geomech.*, **15**(6), 319-368.
- Khavé, G.J. (2014), “Delineating subterranean water conduits using hydraulic testing and machine performance parameters in TBM tunnel post-grouting”, *Int. J. Rock Mech. Min. Sci.*, **70**, 308-317.
- Lisa, H., Christina, B., Åsa, F., Gunnar, G. and Johan, F. (2012), “A hard rock tunnel case study: Characterization of the water-bearing fracture system for tunnel grouting”, *Tunn. Undergr. Space Technol.*, **30**, 132-144.
- Mohajerani, S., Baghbanan, A., Bagherpour, R. and Hashemolhosseini, H. (2015), “Grout penetration in fractured rock mass using a new developed explicit algorithm”, *Int. J. Rock Mech. Min. Sci.*, **80**, 412-417.
- Mohammed, M.H., Pusch, R. and Knutsson, S. (2015), “Study of cement-grout penetration into fractures under static and oscillatory conditions”, *Tunn. Undergr. Space Technol.*, **45**, 10-19.
- Northcroft, I.W. (2006), “Innovative materials and methods for ground support, consolidation and water sealing for the mining industry”, *J. S. Afr. I. Min. Metall.*, **106**(12), 835-844.
- Panthi, K.K. and Nilsen, B. (2010), “Uncertainty for assessing leakage through water tunnels: A case from Nepal Himalaya”, *Rock Mech. Rock Eng.*, **43**(5), 629-639.
- Rafi, J.Y. and Stille, H. (2014), “Control of rock jacking considering spread of grout and grouting pressure”, *Tunn. Undergr. Space Technol.*, **40**, 1-15.
- Rahman, M., Håkansson, U. and Wiklund, J. (2015), “In-line rheological measurements of cement grouts: Effects of water/cement ratio and hydration”, *Tunn. Undergr. Space Technol.*, **45**, 34-42.
- Saberhosseini, E., Keshavarzi, R. and Ahangari, K. (2014), “A new geomechanical approach to investigate the role of in-situ stresses and pore pressure on hydraulic fracture pressure profile in vertical and horizontal oil wells”, *Geomech. Eng., Int. J.*, **7**(3), 233-246.
- Saeidi, O., Stille, H. and Torabi, S.R. (2013), “Numerical and analytical analyses of the effects of different joint and grout properties on the rock mass groutability”, *Tunn. Undergr. Space Technol.*, **38**, 11-25.
- SsangYong cement Inc. (2016), <http://www.ssangyongcement.co.kr/jsp/business/business06-08.jsp>
- Stille, H., Gustafson, G. and Hassler, L. (2012), “Application of new theories and technology for grouting of

- Dams and foundations on rock”, *Geotech. Geol. Eng.*, **30**(3), 603-624.
- Sui, W., Liu, J., Hu, W., Qi, J. and Zhan, K. (2015), “Experimental investigation on sealing efficiency of chemical grouting in rock fracture with flowing water”, *Tunn. Undergr. Space Technol.*, **50**, 239-249.
- Wang, J.-B., Liu, X.-R., Huang, Y.-X. and Zhang, X.-C. (2015), “Prediction model of surface subsidence for salt rock storage based on logistic function”, *Geomech. Eng., Int. J.*, **9**(1), 25-37.
- Yoon, S., Lee, S.-R., Kim, Y.-T. and Go, G.-H. (2015), “Estimation of saturated hydraulic conductivity of Korean weathered granite soils using a regression analysis”, *Geomech. Eng., Int. J.*, **9**(1), 101-113.
- Zhang, G., Zhan, K., Gao, Y. and Wang, W. (2011), “Comparative experimental investigation of chemical grouting into a fracture with flowing and static water”, *Min. Sci. Technol. (China)*, **21**(2), 201-205.
- Zhang, Q., Xu, Z., Wu, J. and He, P. (2017), “Grouting effects evaluation of water-rich faults and its engineering application in Qingdao Jiaozhou Bay Subsea Tunnel, China”, *Geomech. Eng., Int. J.*, **12**(1), 35-52.
- Zhu, H., Guo, J., Zhao, X., Lu, Q., Luo, B. and Feng, Y. (2014), “Hydraulic fracture initiation pressure of anisotropic shale gas reservoirs”, *Geomech. Eng., Int. J.*, **7**(4), 403-430.